



## COMPARATIVE STUDY OF TENSILE PROPERTIES OF HYBRID AA6061/SIC/CARBONIZED COCONUT SHELL MICRO AND NANO COMPOSITES

Michael N. Nwigbo<sup>1\*</sup>, Umoru E. Lasisi<sup>2</sup> and Youngson N. Ukaru<sup>3</sup>

<sup>1</sup>Ph.D Researcher, Department of Mechanical and Aerospace Engineering, University of Uyo, Nigeria

<sup>2</sup>Professor, Department of Materials and Metallurgical Engineering, Obafemi Awolowo University, Nigeria

<sup>3</sup>Department of Mechanical and Aerospace Engineering, University of Uyo, Nigeria

\* Corresponding Email: [nwigbon@yahoo.com](mailto:nwigbon@yahoo.com)

### Cite this article:

Nwigbo M.N., Lasisi U.E., Ukaru Y.N. (2022), Comparative Study of Tensile Properties of Hybrid AA6061/SIC/Carbonized Coconut Shell Micro and Nano Composites. International Journal of Mechanical and Civil Engineering 5(1), 10-24. DOI: 10.52589/IJMCE-YEMPPWEP

### Manuscript History

Received: 31 Jan 2022

Accepted: 23 Feb 2022

Published: 17 March 2022

**Copyright** © 2022 The Author(s). This is an Open Access article distributed under the terms of Creative Commons Attribution-NonCommercial-NoDerivatives 4.0 International (CC BY-NC-ND 4.0), which permits anyone to share, use, reproduce and redistribute in any medium, provided the original author and source are credited.

**ABSTRACT:** *This study synthesized a hybrid aluminium 6061 matrix composite with particulates of silicon carbide, SiC<sub>p</sub> and carbonized coconut shell (CCS<sub>p</sub> as reinforcements), and determined the effect of combining SiC<sub>p</sub> and CCS<sub>p</sub> reinforcements of different sizes and weight fractions on the strength properties and microstructure of the developed composite. The hybrid aluminium matrix composites were developed using the stir casting method. Several samples of the composites consisting of AA6061 alloy with 3, 6, 9, 12 and 15% by wt. each of CCS<sub>p</sub> and SiC<sub>p</sub> with average particle sizes of 38µm and 42.3nm for SiC, and 63µm and 50.01nm for CCS<sub>p</sub> were produced and characterized for strength. The microstructures of the developed composite materials revealed uniform distribution of reinforcement particles in the base matrix and excellent bonding between the base matrix and reinforcements after casting. The results obtained showed that addition of CCS<sub>p</sub> and SiC<sub>p</sub> reinforcement to the alloy increased the tensile strength and hardness. Also, a mathematical model was proposed for predictive tensile strength of nano-composite and validated by comparison with results of the physical experiment and those of other authors. The proposed model is in excellent agreement with experimental data. The nano-particulates reinforced composite presented maximum improvement in ultimate tensile strength value (53.4% and 8.5% of that for the unreinforced matrix and micro-composite respectively) at reinforcement level of 15wt.% nSiC/nCCS.*

**KEYWORDS:** AA6061 alloy, stir casting, metal matrix composites, reinforcements, microstructure, nanoparticles.



## INTRODUCTION

Aluminium alloys find wide applications in industrial practice because of their good combination of high strength, low density, durability, machinability, availability, and cost which is very attractive compared to competing materials. Thus, they are very attractive for lightweight applications such as automobile, aerospace, military and transport sectors due to high specific strength, good fatigue properties and wear resistance (Wang *et al.*, 2014; Karl, 2006). However, the scope of these properties can be extended by using aluminium matrix composites (AMCs). Composite materials technologies present unique opportunity to modify the properties of aluminium. This could include increased strength, decreased weight, higher service temperature, improved wear resistance, higher elastic modulus, controlled coefficient of thermal expansion, improved fatigue properties, etc. (Parswajinan *et al.*, 2018; Sudipt & Ananda, 2008; Michael *et al.*, 2015). The property of the AMCs depends on the property of the matrix and the reinforcement. (Vijaya *et al.*, 2014). The reinforcement in AMCs may be in the structure of continuous fibres, discontinuous fibres, whiskers or particulates. Widely used reinforcement ceramic materials in AMCs include silicon carbides (SiC), titanium borides (TiB<sub>2</sub>), alumina (Al<sub>2</sub>O<sub>3</sub>), nitrides, boron and graphite.

Recently, reinforcements commonly used in aluminium matrix composites have been extended to include agro-wastes such as rice waste ash, palm oil fuel ash, sugar cane bagasse, palm kernel ash, periwinkle shell ash and coconut shell ash (Senthilkumar *et al.*, 2016; Iyasele, 2018). These agro-wastes are cheap and readily available in high quantities. Ajibola and Fakeye (2015) reported the production and characterization of Zinc-Aluminium composite reinforced with silicon carbide and palm kernel shell ash (PKSA), in which samples prepared with compositions 5wt% SiC added with 0.2, 0.4, 0.6, 0.8 and 1.0wt% PKSA were utilized to prepare the reinforcing phase with Zinc-Aluminium matrix composite using two-step stir casting method. The agro waste material was pre-heated to 650<sup>0</sup>C before being introduced into the Zinc-Aluminium composite in molten state. Hardness and tensile test were used to characterize the composite produced. The result shows that increase in PKSA reinforcement increases the hardness and tensile strength of the composite, and the microstructure shows that SiC and PKSA were well dispersed in the alloy matrix.

Hima *et al.* (2018) used aloe vera powder to reinforce the aluminum metal matrix in order to study the mechanical characterization of the AMMC. He compared the suitability of fly ash (reported by several researchers) and aloe vera as reinforcement particulates for the aluminum metal matrix, but his study reported that the use of aloe vera significantly reflected an improvement on the mechanical properties of the AMMC with regards to tensile strength, impact strength, and hardness, compared to the popularly known and used fly ash. Nwobi-Okoye and Ochieze (2018) experimentally studied the behavior of aluminum alloy A356 reinforced with a particulate composite of cow horn, for application in a brake drum via the use of an artificial neural network (ANN), response surface methodology (RSM), and simulated annealing. The study was focused on modeling the age hardness process on the developed or reinforced AMMC using ANN and RSM. The result revealed that the modeling via ANN that generated the data for age hardening was improved by 0.9583 predictions compared with that of RSM of 0.9921 predictions of ANN.

Umunakwe *et al.* (2017) investigated the density, porosity, microstructure and some mechanical properties of particulate periwinkle shell-aluminium 6063 metal matrix composite (PPS-AMMC) produced by two-step casting and compared the properties of the composites



with those of the aluminium 6063 (Al60603) alloy. Periwinkle shells were milled to particle sizes of 75 $\mu$ m and 150 $\mu$ m and used to produce PPS-AlMMC at 1, 5, 10 and 15wt% filler loadings using two-step casting technique. The addition of PPS to aluminium alloy reduced the density of the composite. It was observed that the filler distributes uniformly in the matrix due to the two-step casting technique. The porosities of the composites were within acceptable level of 0–5% except for the composite with 15wt% PPS of 150 $\mu$ m particle size. Improved strength, ductility, hardness and modulus were obtained when the filler was used to reinforce the alloy. However, using a filler of higher particle size resulted in higher porosity, reduced tensile strength, ductility and toughness.

In this work, an attempt has been made to prepare and characterize hybrid AA6061 alloy composites by adding SiC and carbonized coconut shell reinforcement particles into the matrix using a stir casting method.

## MATERIALS AND METHODS

Aluminium alloy 6061 was used as base material; silicon carbide and carbonized coconut shell were used as the reinforcements. Table 1 shows the chemical composition of Al6061 Alloy. The equipment include locally constructed laboratory-size electric furnace, electronic weighing machine, sieve shaker, crucible pot (stainless steel), tongs, hacksaw, lathe machine, extensometer, grinding deck, abrasive papers (220, 400, 600, 800 and 1000 grits), electric dryer, scanning electron microscope, grinding and polishing machines, etc.

The coconut shells were washed with water to remove impurities and dried in an oven at 110<sup>0</sup>C to reduce its moisture content. It was then crushed and grinded to form coconut shell powder. The powder was packed in a graphite crucible and fired in an electric furnace in the absence of air to a temperature of 600<sup>0</sup>C and held for 5 hrs to form carbonized coconut shell ash. In order to further reduce the particle size, the carbonized coconut shell ash was ball milled for 60 hrs in accordance with Bello (2017). After ball milling, the carbonized coconut shell ash was classified for particle size. The silicon carbide particulates were also ball milled for 50 hrs and classified for particle size. Samples of the AA6061/SiC/CCS composites were then fabricated by stir casting method (Figure 1e). The process of stir casting starts with placing empty crucible in the furnace. The base metal is AA6061 alloy and was melted at 700<sup>0</sup>C in a crucible. Simultaneously, reinforcements were preheated to a temperature of 300<sup>0</sup>C to improve the wettability, remove moisture and also to reduce the temperature gradient between molten metal and reinforcements. Magnesium of 2wt% was added to the molten metal to enhance the wettability between reinforcements and molten metal. The molten metal was stirred using a stainless steel stirrer and measured quantity of reinforcement was added. The mixture was stirred for 5 minutes for uniform distribution. Then molten metal was poured in a sand mould and allowed to solidify. The same procedure was repeated for fabrication of composites with different weight percentage of reinforcements of 0, 3, 6, 9, 12 and 15%wt of CCS and SiC respectively and different particle sizes.

**Table 1: Composition of AA6061**

| Element  | Si    | Fe    | Cu    | Mn    | Mg    | Ni    | Zn    | Ti    | Cr    | Al   |
|----------|-------|-------|-------|-------|-------|-------|-------|-------|-------|------|
| Weight % | 0.514 | 0.230 | 0.161 | 0.071 | 0.960 | 0.010 | 0.015 | 0.031 | 0.103 | Bal. |

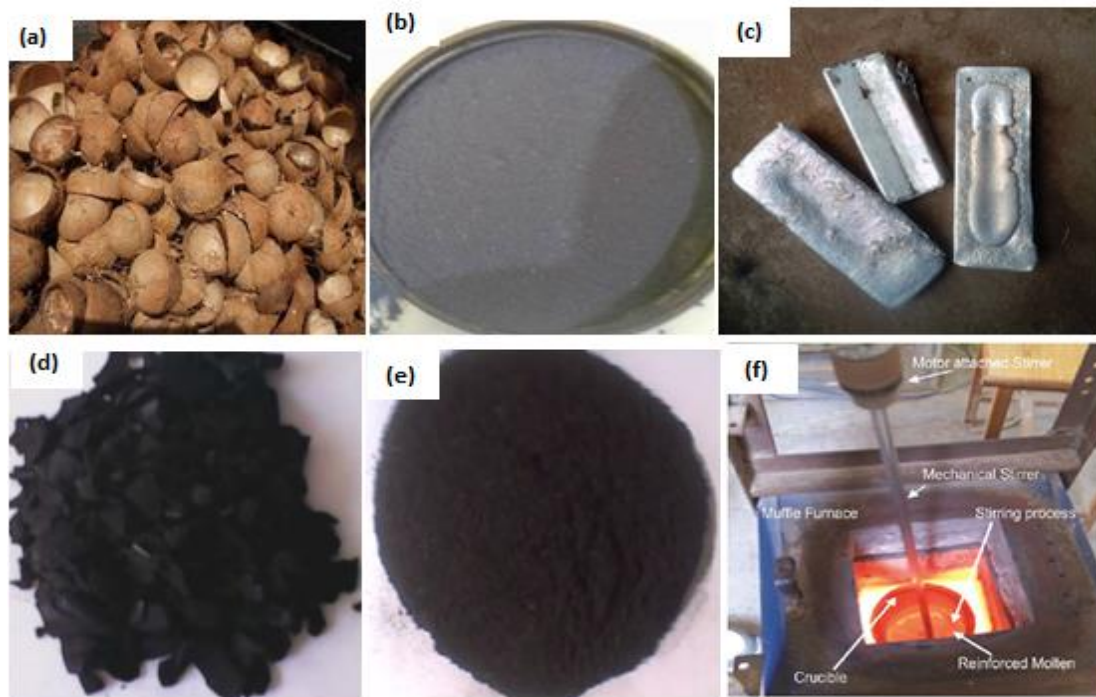


**Figure 1: (a) Coconut shells (b) Silicon carbide (c) Cast AA6061 ingot (d) Crushed carbonized Coconut shells (e) Carbonized coconut particulates (f) Stir casting furnace**

### Tensile Testing

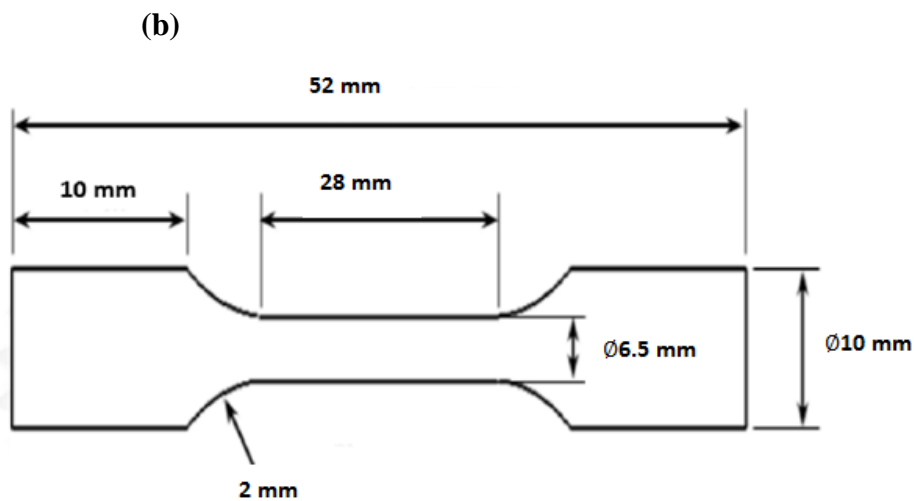
The tensile test was carried out on the composite samples to determine its strength and ductility, yield strength and other tensile properties. In the present investigation all the tensile tests were conducted using Monsanto Tensometer {type W, serial 11148} tensile test machine at the Department of Materials and Metallurgical Engineering, Federal University of Technology, Owerri. The standard tensile test sample of a dumbbell shape with a diameter of 6.5 mm and gauge length 28 mm was used for the research. An initial load of 5kN was applied on the samples; this load was increased until failure occurred. The specimen was axially loaded in tension; the distance between the gauge marks was monitored. The specimen was elongated by the moving crosshead; load cell and extensometer measured the magnitude of the load and the elongation. All tests are conducted at room temperature.



(a) Tensometer



(b) Test specimens



(c) Test specimen with dimensions

**Figure 2: Tensile test set up**

### Modeling Tensile Strength

To validate the experimental response of the overall AMC property, it is important to incorporate realistic material properties in the model representation. In the current study, the aluminum matrix is assumed to be an elastic-plastic material and the inclusions are approximated as being made of spherical and linear elastic silicon carbide and carbonized coconut shell particulates. The interface between the matrix and the inclusions is assumed to be ideal and particle cracking is not considered. Analytical model established by Pankanszky *et al.* (1988) gives an empirical relationship between strength of composite ( $\sigma_c$ ) and strength of matrix ( $\sigma_m$ ) as given in Equation 1:



$$\sigma_c = \left[ \sigma_m \left( \frac{1-V_p}{1+2.5V_p} \right) \right] e^{BV_p} \quad (1)$$

where an empirical constant B is dependent on particle surface area, interfacial bonding strength, and particle density. The B value varies in between 3.49 to 3.87. The Pankanzky empirical relationship, as given in Equation 1, gives the ultimate strength of the particulate metal matrix composite which is dependent on the strong particle-matrix interfacial bonding. While considering the Pankanzky's empirical relationship, necessary care has been taken about the particulate involvement in composite and interfacial bonding between the nanoparticles/matrix, particle size, precipitate formation, agglomeration, voids/porosity and dislocation barriers.

Also, considering adhesion, precipitate formation, particle size, agglomeration, voids/porosity, dislocation obstacles and the particle/matrix interfacial reaction, modified Voigt model considering these factors may be expressed as:

$$\underline{\sigma}_c = V_m \underline{\sigma}_m + \sum_{j=1,2, \dots, n} \{ V_{r_j} \underline{\sigma}_{r_j} + \varepsilon_f \} \quad \underline{\varepsilon}_c = V_m \underline{\varepsilon}_m + \sum_{j=1,2, \dots, n} \{ V_{r_j} \underline{\varepsilon}_{r_j} + \varepsilon_f \} \quad (2)$$

where  $\underline{\sigma}_c$ ,  $\underline{\sigma}_m$  and  $\underline{\sigma}_{r_j}$  are the composite, matrix and reinforcement strength respectively and  $\underline{\varepsilon}_c$ ,  $\underline{\varepsilon}_m$  and  $\underline{\varepsilon}_{r_j}$  are the corresponding strains. The volume fractions of matrix material and reinforcement are respectively  $V_m$  and  $V_{r_j}$ . The term  $\varepsilon_f$  is a correction factor accounting for the effect of reinforcement particle size, porosity and interfacial interaction, and is determined from experimental data of the composite.

In this study, the matrix material is reinforced with two different types of particulates; thus, Equation 2 is rewritten as:

$$\underline{\sigma}_c = V_m \underline{\sigma}_m + V_{r_1} \underline{\sigma}_{r_1} + V_{r_2} \underline{\sigma}_{r_2} + \varepsilon_f \underline{\varepsilon}_c = V_m \underline{\varepsilon}_m + V_{r_1} \underline{\varepsilon}_{r_1} + V_{r_2} \underline{\varepsilon}_{r_2} + \varepsilon_f \} \quad (3)$$

But  $V_m + V_{r_1} + V_{r_2} = 1$

$$\Rightarrow V_m = 1 - (V_{r_1} + V_{r_2})$$

where,  $V_m$ ,  $V_{r_1}$  and  $V_{r_2}$  are the volume fractions of the matrix and the two different particulates 1 and 2 respectively.



The modified load transfer effect according to Sanaty-Zadeh (2012) is given as:

$$\Delta\sigma_{LT} = \frac{1}{2}V_p\sigma_m \quad (4)$$

and the Hall-Petch strengthening equation as modified by Hull and Bacon (2001) is:

$$\Delta\sigma_{H-P} = \frac{k_y}{\sqrt{d}} \quad (5)$$

Combining Equations 4 and 5, and neglecting the volume fractions of voids/porosity gives Equation 6:

$$\sigma_c = \frac{1}{2}V_p\sigma_m + \frac{k_y}{\sqrt{d_p}} \quad (6)$$

For matrix material reinforced with n different particulates, Equation 6 becomes:

$$\sigma_c = \frac{1}{2}\left(\sum V_{p_i}\right)\sigma_m + \frac{k_y}{\sqrt{\left(\sum d_{p_i}\right)}} \quad \{i = 1, 2, n\} \quad (7)$$

For matrix material reinforced with two different particulates, Equation 3.36 becomes:

$$\sigma_c = \frac{1}{2}(V_{p_1} + V_{p_2})\sigma_m + \frac{k_y}{\sqrt{(d_{p_1} + d_{p_2})}} \quad (8)$$

Table 2 gives the material data for models prediction.

**Table 2: Material and model parameters**

| Material                           | Elastic modulus<br>(GPa) | Tensile strength<br>(MPa) | Density<br>(g/cm <sup>3</sup> ) | Poisson ratio |
|------------------------------------|--------------------------|---------------------------|---------------------------------|---------------|
| Silicon carbide                    | 410                      | 336                       | 3.21                            | 0.14          |
| Carbonized coconut shell particles | 512                      | 18.03                     | 1.68                            | 0.92          |
| AA6061                             | 69                       | 162.6                     | 2.72                            | 0.33          |

## RESULTS AND DISCUSSION

### Tensile and Yield Strength of Hybrid AA6061/SiC/CCS Composites

Figures 3 and 4 show progressive improvement in ultimate tensile and yield strength values for hybrid micro and nano composites. The ultimate tensile and yield strengths of the composites were observed to continuously improve as the percentage of the particles was increased. This improvement continues with decreasing reinforcement particulate size. This is evident as the hybrid nano-composites acquired superior ultimate tensile and yield strengths than the hybrid micro-composites. Similar trend has been reported in literature (Prasad & Krishna, 2010; Abba-Aji, 2021; Michael, 2022). Donald *et al.* (2018) and Padmavathi and Ramakrishnan (2019) also reported improved tensile strength properties of AMC composite. The observed increase in strength value is attributed to the matrix phase refinement and the integration of hard and brittle phases of micro and nano- particles of silicon carbide ( $\mu\text{SiC}$  and  $\text{nSiC}$ ),  $\text{SiO}_2$ ,  $\text{Al}_2\text{O}_3$  and  $\text{Fe}_2\text{O}_3$  (obtained from micro- and nano-particles of carbonized coconut shell,  $\mu\text{CCS}$  and  $\text{nCCS}$  in the matrix material. The hard and brittle phases constitute barriers to dislocation movement across the grain boundaries. This in effect strengthens the soft matrix and improves the hardness of their composites.

Another factor that may contribute to the better interaction between the particles and the matrix is the clean and clear interface between them, conferring the composite an increased load-carrying capacity. Composites with 15wt.%  $\text{nSiC/nCCS}$  and 15wt.%  $\mu\text{SiC}/\mu\text{CCS}$  presented maximum improvement in ultimate tensile strength value (53.4% and 41.5% respectively, for  $\text{nSiC/nCCS}$  and  $\mu\text{SiC}/\mu\text{CCS}$ ) compared to the base alloy. Another possible reason for the improved ultimate tensile strength value could be the interaction between the particles and dislocations when the composites are under load; it could also be due to the existence of several appending dislocations around the particles owing to the variation in the thermal expansion coefficient between the particles and the base matrix. The mismatch in thermal expansion coefficient between the matrix and the particles will also strengthen dislocation at the grain boundary based on the level of mismatch. The increase in yield strength was due to the decreased inter-particle spacing between the SiC and CCS particles as the particles are harder than the base alloy. Also, the addition of micro and nano particulates of SiC and CCS to the base alloy suppressed stress deformation, thereby improving the yield strength of the composites.



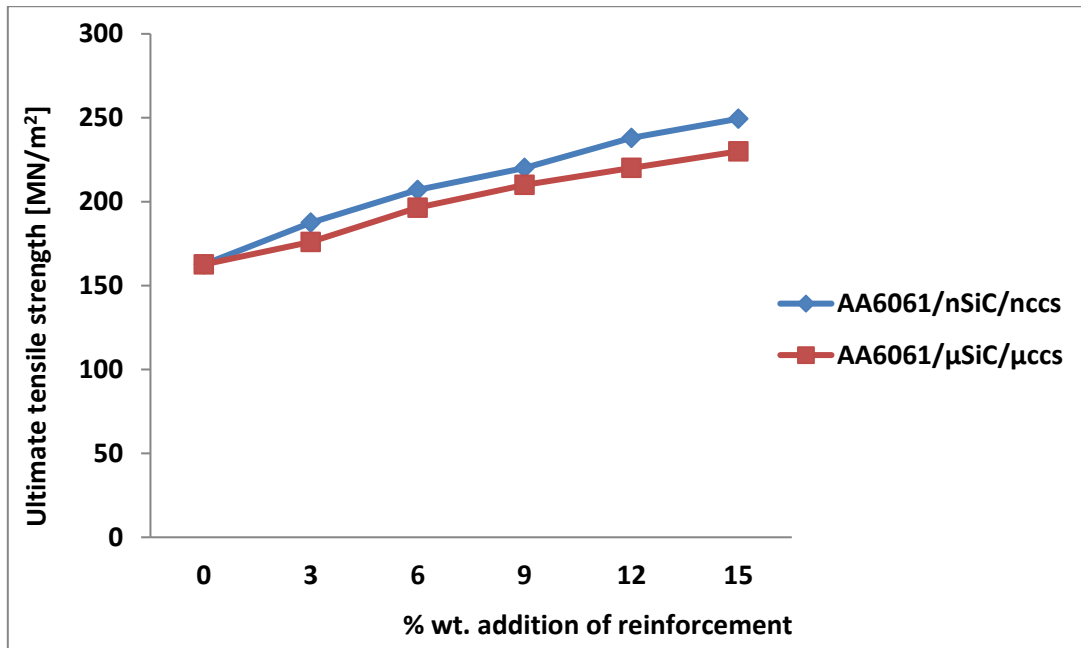


**Figure 3: Ultimate tensile strength of Hybrid AA6061/SiC/CCS Micro and Nano Composites**

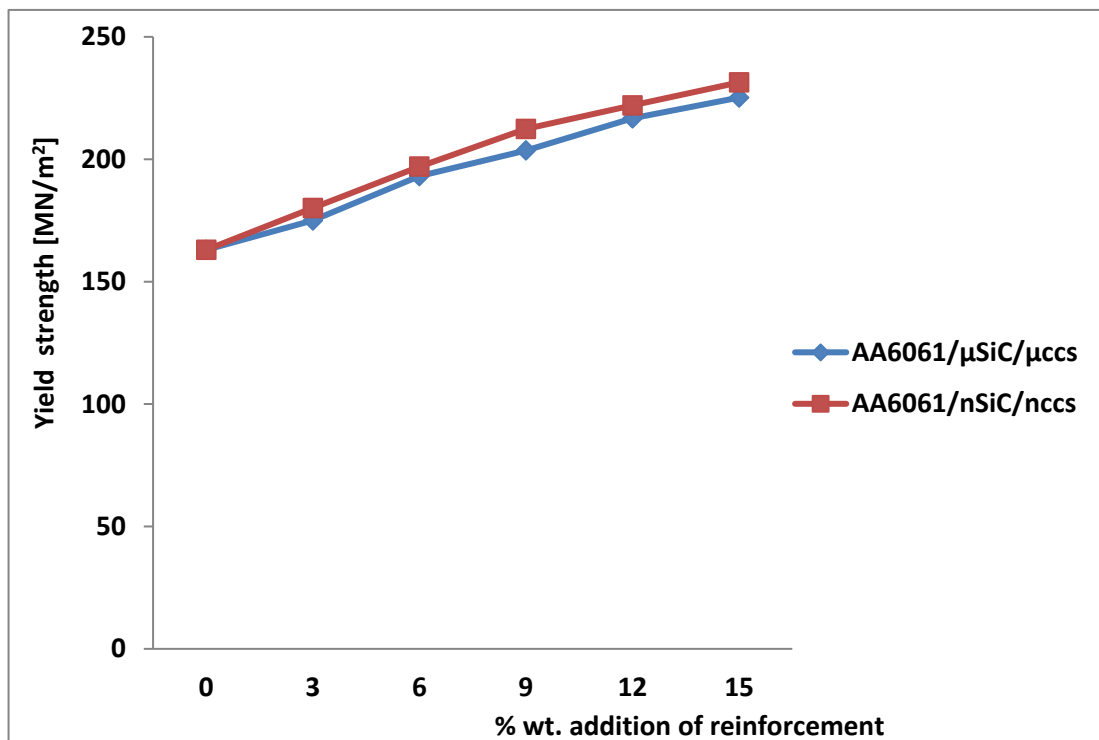


**Figure 4: Yield strength of Hybrid AA6061/SiC/CCS Micro and Nano Composite**



### Modeling of Tensile Strength of Hybrid AA6061/SiC/CCS Nano Composites

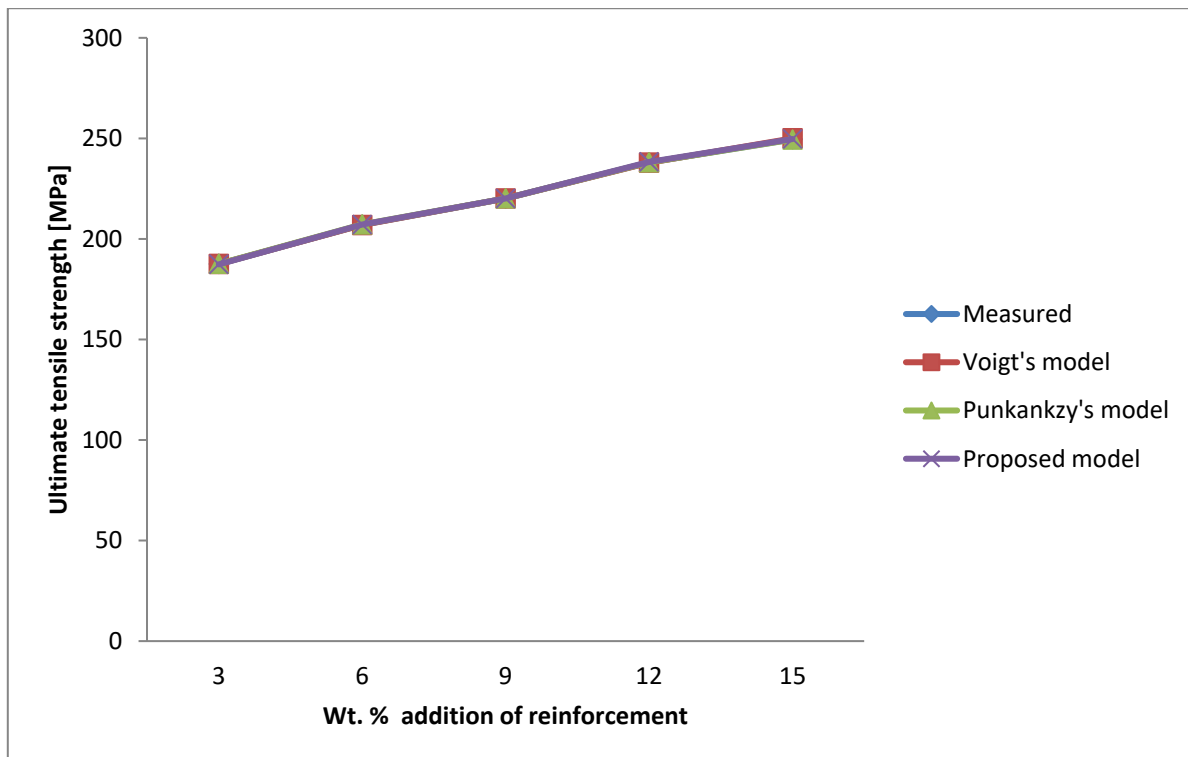
The experimental data for composite strength, accompanied by mathematical model predictions from earlier works and present study are shown in Table 3 and Figure 5. Widely used models for the prediction of composite strength and the proposed model are listed in Table 4.

Table 3 and Figure 5 indicate that the results of the predictions by the proposed model in this work are in excellent agreement with those of the experimental data—Voigt's model and Punkankzy's model—and thus validates its suitability for tensile strength prediction of particle reinforced hybrid metal matrix composites. Further, it was observed that the popular Voigt's model gives significantly higher values than the measured values and those by Reddy and the present work. This is because the Voigt's model does not take into account the effect of reinforcement particle size, porosity and interfacial reactions in the composite. However, a modified Voigt model was developed by introducing a correction factor that accounts for the effect of particle size, porosity and interfacial interactions that was determined from the experimental data of the composite. Hence, the results of the modified Voigt model given in Table 3 are consistent with those of the experimental data (Punkankzy's model) as well as the proposed model.

**Table 3: Comparison of experimental and model predicted composite strength**

| S/N | Wt.% of nSiC and nCCS | Measured $\sigma_c$ (MPa) | Modified Voigt's model     |                            | Punkankzy's model          |                            | Proposed model             |                            |
|-----|-----------------------|---------------------------|----------------------------|----------------------------|----------------------------|----------------------------|----------------------------|----------------------------|
|     |                       |                           | Predicted $\sigma_c$ (MPa) | Residuals $\sigma_c$ (MPa) | Predicted $\sigma_c$ (MPa) | Residuals $\sigma_c$ (MPa) | Predicted $\sigma_c$ (MPa) | Residuals $\sigma_c$ (MPa) |
| 1   | 6                     | 187.5                     | 187.51                     | 0.01                       | 187.60                     | 0.10                       | 187.34                     | - 0.16                     |
| 2   | 12                    | 207.0                     | 206.90                     | - 0.10                     | 207.20                     | 0.20                       | 207.12                     | - 0.12                     |
| 3   | 18                    | 220.1                     | 220.10                     | 0.00                       | 220.14                     | 0.04                       | 220.09                     | - 0.01                     |
| 4   | 24                    | 238.0                     | 237.90                     | - 0.10                     | 238.04                     | 0.04                       | 238.28                     | 0.28                       |
| 5   | 30                    | 249.5                     | 250.00                     | 0.50                       | 249.40                     | - 0.10                     | 249.68                     | 0.18                       |

The value of strength constant  $k_y$  for the proposed model (see Table 4) as determined from experimental data ranges from  $3.92 \times 10^{-3}$ MPa (at 6wt.% addition of nSiC and nCCS) to  $4.48 \times 10^{-3}$ MPa (at 30wt.% addition of nSiC and nCCS) while the correction factor for the modified Voigt's model ranges from 24.04 to 82.58 MPa for reinforcement addition ranging from 6wt.% to 30 wt. % addition of nSiC and nCCS. Also, the B value in Punkankzy's model varies in between 4.48 to 5.74 in decreasing amount of reinforcement addition in contrast with the stated range of 3.49 to 3.87 as given by Punkankzy. The variation in B values compared with those of Punkankzy was attributed to non-inclusion of effect of precipitate formation, agglomeration, voids/porosity and dislocation barriers in the response computation.



**Figure 5: Comparative plots of hybrid nano-composite strength obtained from model prediction**

**Table 4: Models for prediction of composite strength**

| S/N | Author(s)    | Model  | Equation |
|-----|--------------|--|----------|
| 1   | Voigt        | $\sigma_c = V_m \sigma_m + \sum V_{r_j} \sigma_{r_j} + \epsilon_f \quad \{j = 1, 2, \dots, n\}$  | 3        |
| 2   | Punkankzy    | $\sigma_c = \left[ \sigma_m \left( \frac{1 - (\sum V_{p_i})}{1 + 2.5(\sum V_{p_i})} \right) \right] e^{B(\sum V_{p_i})} \quad \{i = 1, 2, n\}$ | 1        |
| 3   | Present work | $\sigma_c = \frac{1}{2} (\sum V_{p_i}) \sigma_m + \frac{k_y}{\sqrt{(\sum d_{p_i})}} \quad \{i = 1, 2, n\}$                                     | 7        |

However, comparative analysis of the composite strength precisely obtained from experiment and predictive models shows that the model-predicted values, deviated from experimental results, as presented in Figure 5. The maximum tolerable deviations (residuals) of model predictions from experimental data were 0.2%, 0.1% and 0.12% for Voigt's model,

Punkankzy's model and the proposed model respectively. The observed deviations are caused by the effect of other process parameters such as stirring speed, stirring temperature, particle agglomeration, melt/mould interactions (reactions), etc. which were ignored during the model development and evaluations. It can therefore be concluded that the proposed model is suitable for prediction of tensile strength of nano-particulate composites with some modifications. The modifications may be the introduction of error factor that will account for the various process parameters affecting the measured response (strength), which can be determined from experimental data for nanocomposite composition.

### Microstructure of Hybrid AA6061/nSiC/nCCS Composites

The SEM micrographs of the AA6061 alloy and those of the composites are shown in Figure 6. Figure 6(a) shows the micrograph of the unreinforced alloy revealing the white  $\alpha$  -phase with equiaxed grain shape (Boppana *et al.*, 2020). Fine grains are found dissipated along as far as possible in the structure of AA6061 alloy. The result of SEM for microstructural examination of the specimens revealed fairly uniform distribution of nSiC and nCCS in the matrix in all %wt addition of the reinforcements (Figure 6b-d).

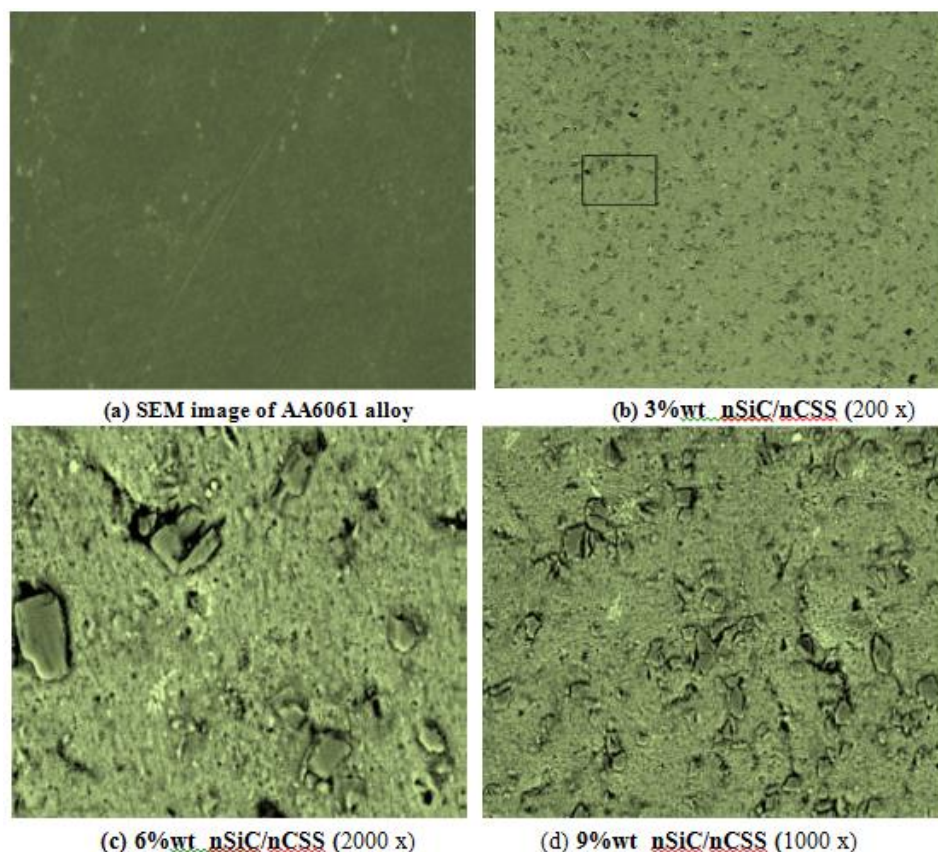


**Figure 6: SEM images of hybrid AA 6061/nSiC/nCCS composites**



The uniform distribution of nSiC and nCCS particles in the matrix can be attributed to a number of factors which include effective stirring of the melt, degassing tablet used and good wettability that resulted in improved interfacial bonding between the matrix and the coconut shell ash particles (Apasi *et al.*, 2016). No segregation of nSiC and nCCS particles were found along the grain boundaries. Distribution of particles was observed to be intra-granular, in which the majority of the particles are located inside the grains. This distribution is preferred in AMCs to have better mechanical and tribological properties. Silicon carbide and carbonized coconut nanoparticles were thermodynamically stable, and there were no pores or voids around them. The reinforcement particles resisted aluminium grain growth and resulted in nucleation sites growth, which led to the formation of finer grains. As the concentration of nSiC and nCCS particles increased in the matrix, composite properties such as hardness, UTS, and resistance to wear also showed improvement.

## CONCLUSION

The hybrid AA6061/SiC/CCS composites have been successfully produced by stir casting method and characterized for analysis of tensile strength and microstructural properties. The effect of reinforcement particulates size and volume fraction on the tensile strength and microstructure of the AA6061/SiC/CCS composites were also investigated. From the analysis of results obtained during this study, the following conclusions were made:

1. The microstructure analysis of the composites revealed a uniform distribution of the reinforcement particles in the matrix. This resulted in excellent bonding properties and grain refinement.
2. The incorporation of the silicon carbide and coconut shell particulates into the aluminium alloy matrix increased the ultimate tensile and yield strength values of the composites.
3. The ductility of AA6061/SiC/CCS composites decreased as the weight fraction of CCS and SiC particles increased.
4. The hybrid AA6061/SiC/CCS nano-composites acquired superior tensile strength properties than the hybrid micro-composite and the matrix alloy.
5. The nano-particulates reinforced composite presented maximum improvement in ultimate tensile strength value (53.4% of that the unreinforced matrix) at reinforcement level of 15wt.% nSiC/nCCS.
6. The composites can be used in areas where higher strength to weight ratio is required within the aerospace, automotive and electronic industries such as cylinder liners in engines, aluminium calipers and power electronic modules.



## REFERENCES

- Abba-Aji, M. A. (2021), Development of Car Piston Material from Aluminium alloy using Coconut shell ash as an additive. PhD Thesis, Department of Industrial and Production Engineering, Federal University of Technology, Minna, Nigeria
- Ajibola, W.A. and Fakeye, A.B. (2015), Production and Characterization of Zinc-Aluminium, Silicon Carbide Reinforced with Palm Kernel Shell Ash, *Int. J. Eng. Trends and Tech. (IJETT)*, 41(6), 318 – 325.
- Bello Sefiu Adekunle (2017) Development and Characterisation of Epoxy-Aluminium-Coconut shell particulate hybrid nanocomposite for automobile applications, PhD Thesis, Department of Metallurgical and Materials Engineering, University of Lagos, Nigeria.
- Boppana, S. B., Dayanand, S., Kumar, A., Kumar, V. and Aravinda, T (2020). Synthesis and characterization of Nano graphene and ZrO<sub>2</sub> reinforced AA6061 metal matrix composites. *J. Mater. Res. Technol.* 2020, 9, 7354–7362.
- Donald, A.O., Hassan, M.A., Hamza, S., Garba, E., Dangtim, D.K. and Mamadou, M. (2018), Development and Characterization of Aluminum Matrix Composites Reinforced with Carbonized Coconut Shell and Silicon Carbide Particle for Automobile Piston Application, *Global Scientific Journals*, 6(8), 390 – 398.
- Hima, G. C., Durga P. K. G., Ramji, K. and Vinay, P. V. (2018), Mechanical Characterization of Aluminium Metal Matrix Composite Reinforced with Aloe vera powder, *Mater. Today*, 5, 3289–3297.
- Hull, D and Bacon, D.T. (2001), *Introduction to Dislocations*, 4th Edition; Butterworth Einmemann; Oxford, U.K.
- Iyasele, E. Omondiale (2018), Comparative Analysis On The Mechanical Properties Of A Metal- Matrix Composite (Mmc) Reinforced With Palm Kernel/Periwinkle Shell Ash, *Global Scientific Journal*, 6(8) 1 – 24.
- Karl, U. Kainer, (2006) *Metal Matrix Composites. Custom-made Materials for Automotive and Aerospace Engineering*, WILEY-VCH Verlag GmbH & Co. KGaA, Weinheim.
- Michael, O. B., Kenneth, K. A. and Lesley, C. (2015), Aluminium matrix hybrid composites: A review of reinforcement philosophies; mechanical, corrosion and tribological characteristics, *J. Mater. Research and Technol.*, 4(4) 434–445.
- Michael, N. Nwigbo (2022), Synthesis and Characterization of Hybrid Aluminium Matrix Composites Reinforced with Silicon Carbide and Carbonized Coconut Shell Particulates for Automotive Applications, PhD Thesis, Department of Mechanical and Aerospace Engineering, University of Uyo, Nigeria.
- Nwobi-Okoye, C. C. and Ochieze, B. Q. (2018), Age hardening process modeling and optimization of Aluminium alloy A356/Cow horn particulate composite for brake drum application using RSM, ANN and simulated annealing. *Def. Technol.*, 14, 336–345
- Padmavathi and Ramakrishnan (2019), Wear Studies on the Heat Treated Al6061- $\mu$ SiC and Al6061- nSiC Metal Matrix Composites, *Intl. J. Mech. Engg and Tech.*, (10) 6, 241-247.
- Parswajinan, C., Vijaya, B. R., Abishe, B., Niharishsagar, B. and Sridhar, G. (2018), Hardness and impact behaviour of aluminium metal matrix composite, *The 3rd International Conference on Materials and Manufacturing Engineering 2018, IOP Conf. Series: Materials Science and Engineering* 390 (2018) 012075.



- Prasad, N. (2006), Development and characterization of metal matrix composite using red Mud an industrial waste for wear resistant application, PhD thesis Department of Mechanical Engineering, National Institute of Technology Rourkela -769 008 (India) January, pp 23-34.
- Sanaty-Zadeh, A. (2012), Comparison between current models for the strength of particulate-reinforced metal matrix nanocomposites with emphasis on consideration of Hall–Petch effect. *Mat. Sci. Eng. A*, 531, 112–118.
- Senthilkumar, G., Manoharan, S., Balasubramanian, K. and Dhanasakkaravarthi, B. (2016), An Experimental Investigation of Metal Matrix Composites of Aluminium (Lm6), Boron carbide and Fly ash, *Australian Journal of Basic and Applied Sciences*, Vol. 10(1), 137-144.
- Sudipt Kumar and Ananda Theerthan J. (2008), Production and Characterisation of Aluminium-Fly Ash Composite Using Stir Casting Method, B. Tech. Project, Department of Metallurgical & Materials Engineering National Institute of Technology, Rourkela.
- Umunakwe, R., Olaleye, D. J., Oyetunji, A., Okoye, O. C. And Umunakwe, I. J. (2017), Assessment of the Density and Mechanical Properties of Particulate Periwinkle Shell-Aluminium 6063 Metal Matrix Composite (PPS-AIMMC) Produced by Two-Step Casting, *ACTA TECHNICA CORVINIENSIS – Bulletin of Engineering Tome X [2017] Fascicule 1 [January – March]*.
- Vijaya, R. B., Elanchezhian, C., Annamalai, R. M., Aravind, Sri Ananda, A. S. T., V. Vignesh, V. and Subramanian, C. (2014) Aluminium Metal Matrix Composites - A Review, *Rev. Adv. Mater. Sci.* 38(2014) 55 – 60.
- Wang, Z., Prashanth, K.G., Scudino, S., Chaubey, A.K., Sordelet, D.J., Zhang, W.W., Li, Y.Y. and Eckert, J. (2014). Tensile properties of Al matrix composites reinforced with in situ  $Al_{84}Gd_6Ni_7Co_3$  glassy particles. *J. Alloy. Compd.* 2014, 586, S419–S422.